Inorganic Chemistry
Article

Inorg. Chem. **2009**, *48*, 8173–8179 **8173**
DOI: 10.1021/ic9003609

Combined Mössbauer Spectral and Density Functional Theory Determination of the Magnetic Easy-Axis in Two High-Spin Iron(II) 2-Pyrazinecarboxylate Complexes

Gary J. Long*

Department of Chemistry, Missouri University of Science and Technology, University of Missouri, Rolla, Missouri 65409-0010

Stefania Tanase

Leiden Institute of Chemistry, Gorlaeus Laboratories, Leiden University, PO Box 9502, NL-2300 RA Leiden, The Netherlands

Françoise Remacle, Ganga Periyasamy, and Fernande Grandjean

Departments of Chemistry and Physics, University of Liège, B-4000 Sart Tilman, Belgium

Received February 22, 2009

A combination of density functional theory (DFT) calculations and Mössbauer spectroscopy has been used to determine that the magnetic easy-axis is coincident with its crystallographic *c*-axis in $[Fe(pca)_2(py)_2]\cdot py$, where pac is the 2-pyrazinecarboxylate ligand. This easy-axis bisects the approximately axial O−Fe−O coordination axes of molecules adjacent to each other along the *b*-axis. In $\{[Fe(pca)_2(H_2O)]\cdot H_2O\}_n$ the easy magnetic axis is not coincident with any of its crystallographic axes nor with the Fe−O(water) coordination axis, but is coincident with one of the Fe···Fe axes in the crystal structure. The DFT calculations, which use the B3LYP functional and the 6-311++G(d,p) basis set, yield s-electron probability densities and electric field gradient tensors for the iron(II) ion that are in excellent agreement with the observed iron-57 Mössbauer spectral isomer shifts and quadrupole interactions. The gas phase results are very similar for calculations based either on the X-ray structures of the two complexes or on their optimized structures; the optimized structures indicate that the iron to ligand bond distances increase in the absence of any solid-state lattice interactions. The results of a normal coordinate vibrational mode analysis of the two optimized structures are compared with the observed infrared spectra.

Introduction

It is often useful, even important, to know the magnetic easy-axis of a magnetically ordered compound. Unfortunately, this information is often difficult to obtain as it requires a magnetic study of an orientated single crystal, often measured along several directions, to fully determine the easy-axis orientation relative to the crystal structure. The problem is even more difficult if the unit cell is monoclinic or triclinic and/or if there is no obvious relationship between the crystal morphology and the molecular structure of the compound under study. Of course, single-crystal or powder neutron diffraction studies[1−3] can also be used to determine the magnetic easy-axis of a compound, but this technique usually requires either a rather large single crystal or as much as a gram of powder and is often hindered by incoherent scattering from any hydrogen present or neutron absorption by any element present with a high neutron absorption cross-section.[4] Fortunately, the iron-57 Mössbauer spectroscopy provides an alternative approach for determining the magnetic easy-axis of an iron containing compound even for an unoriented microcrystalline compound.

To a first approximation, that is, if the electric field perturbation is smaller than that of the magnetic field,[5,6] the four inner lines of an iron-57 Mössbauer spectral magnetic sextet are shifted relative to the center of the two outer lines by a quadrupole shift, QS, a shift that depends upon the

*To whom correspondence should be addressed. E-mail: glong@mst.edu.

(1) Bacon, G. E. *Neutron Diffraction*; Clarendon Press: Oxford, 1975.
(2) Williams, W. G. *Polarized Neutrons*; Clarendon Press: Oxford, 1988.
(3) *Chemical Applications of Thermal Neutron Scattering*; Willis, B. T., Ed.; Oxford University Press: Oxford, 1973.
(4) Yelon, W. B. In *Interstitial Intermetallic Alloys*; Grandjean, F., Long, G. J., Buschow, K. H. J., Eds.; Kluwer Acad. Publ.: Dordrecht, 1995; pp 225−248.
(5) Ingalls, R. *Phys. Rev.* **1964**, *133*, A787.
(6) Greenwood, N.; Gibb, T. *Mössbauer Spectroscopy*; Chapman and Hall: London, 1971.

Published on Web 07/24/2009

angle, θ, between the easy-axis of magnetization, that is assumed to be parallel to the hyperfine field, and the principal axis of the electric field gradient tensor through the relationship,

$$QS = \Delta E_Q(3\cos^2\theta - 1)/2$$

where ΔE_Q is the electric quadrupole interaction, often referred to as the iron-57 quadrupole splitting, and is given by

$$\Delta E_Q = \frac{1}{2}eQV_{zz}\sqrt{1+\frac{\eta^2}{3}}$$

where e is the electron charge, Q is the nuclear quadrupole moment, V_{zz} is the principal component of the electric field gradient tensor, and η is its asymmetry parameter.[6] The magnitude of ΔE_Q may be determined from the paramagnetic spectrum obtained above the ordering temperature. Hence, from a measurement of QS in the magnetic spectrum and of ΔE_Q in the paramagnetic spectrum, the angle, θ, between the easy-axis of magnetization and the principal axis of the electric field gradient can be determined.

If the electric and magnetic field perturbations are comparable and/or the asymmetry parameter[7] of the electric field gradient is non-zero, the positions of the eight possible lines of an iron-57 Mössbauer spectrum can be obtained by obtaining the eigenvalues of the ground and excited state Hamiltonians for the iron-57 nucleus, positions that depend on the magnetic hyperfine field, H, the principal component of the electric field gradient tensor, V_{zz}, its asymmetry parameter, η, and the Euler angles, θ and ϕ, that define the orientation of the magnetic field, H, in the principal axes of the electric field gradient tensor.

Herein, we use Mössbauer spectral results to determine θ and density functional theory (DFT) to determine the electric field gradient tensor experienced by the iron-57 nucleus. This information then yields the magnetic easy-axis of an ordered compound, if, as is usually the case, the magnetic moment is aligned parallel with the hyperfine field experienced by the iron-57 nucleus.

To evaluate this approach we have chosen to study two iron(II) complexes, $[Fe(pca)_2(py)_2]\cdot py$, **1**, and $\{[Fe(pca)_2(H_2O)]\cdot H_2O\}_n$, **2**, where pca is the 2-pyrazinecarboxylate anionic ligand and py is pyridine.[8] These two complexes were chosen for an initial study for several reasons. First, we wanted to determine the orientation of the principal axis of the electric field gradient in the compounds, and the orientation of this axis seemed rather certain in **1** but uncertain in **2**. Second, they contained no heavy metals that would impede any computation. Third, their magnetic Mössbauer spectra obtained at 4.2 K were clearly influenced by the orientation, what ever it was. Fourth, the molecular and crystallographic structures of these complexes were known, see Figures 1 and 2. These complexes are paramagnetic above 12 K, are antiferromagnetically ordered below 12 K, and exhibit[8] fully ordered Mössbauer spectra at 4.2 K, see Figure 3. Because the electric field and magnetic field

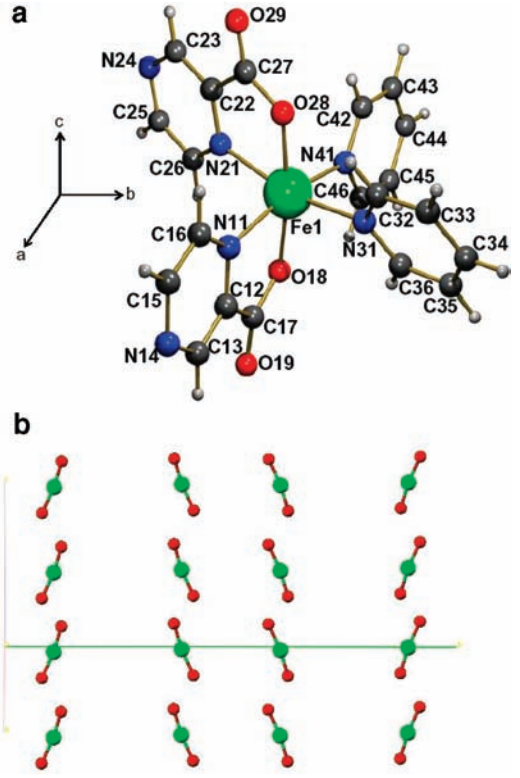

Figure 1. Molecular (a) and the partial crystallographic structure (b) obtained from reference 8, of $[Fe(pca)_2(py)_2]$, **1**, in $[Fe(pca)_2(py)_2]\cdot py$. The iron(II) ion is shown in green, oxygen in red, nitrogen in blue, carbon in black, and hydrogen in gray. In (b) the green line is the *b*-axis, the *c*-axis points up in the plane of the figure, and the *a*-axis makes an angle of 118.9° with respect to the *c*-axis.

perturbations are in an approximately 1:2 ratio in both complexes, the fits shown in Figure 3 have been obtained from the eigenvalues and eigenvectors of the ground and excited state Hamiltonians mentioned above. It is apparent from Figure 3, and the corresponding hyperfine parameters,[8] that the spectra of these two complexes are very sensitive to the angle θ.

The following results are, of course, constrained by the structural aspects of complexes **1** and **2**. Further, although the use of complexes **1** and **2** may not provide the most definitive possible test for the general determination of the orientation of the magnetic easy axis, our success does point the way to the future applications of DFT to related, perhaps more complex, compounds.

Computational Methods

DFT calculations with the Gaussian03 quantum chemical program[9] have been carried out with the B3LYP functional

(7) Grandjean, F.; Long, G. J. In *Interstitial Intermetallic Alloys*; Grandjean, F.; Long, G. J.; Buschow, K. H. J., Eds.; Kluwer Acad. Publ.: Dordrecht, 1995; pp 463−496.

(8) Tanase, S.; Marqués Gallego, P.; Bouwman, E.; Long, G. J.; Rebbouh, L.; Grandjean, F.; de Gelder, R.; Mutikainen, I.; Turpeinen, U.; Reedijk, J. *J. Chem. Soc., Dalton Trans*. **2006**, 1675.

(9) Frisch, M. J.; Trucks, G. W.; Schlegel, H. B.; Scuseria, G. E.; Robb, M. A.; Cheeseman, J. R.; Zakrzewski, V. G.; Montgomery, J. A.; Stratmann, R. E.; Burant, J. C.; Dapprich, S.; Millan, J. M.; Daniels, A. D.; Kudin, K. N.; Strain, M. C.; Farkas, O.; Tomasi, J.; Barone, V.; Cossi, M.; Cammi, R.; Mennucci, B.; Pomelli, C.; Adamo, C.; Clifford, S.; Ochterski, J.; Peterson, G. A.; Ayala, P. Y.; Cui, Q.; Morokuma, K.; Malick, D. K.; Rabuck, A. D.; Raghavachari, K.; Foresman, J. B.; Cioslowski, J.; Ortiz, J. V.; Stefanov, B. B.; Liu, G.; Liashenko, A.; Piskorz, P.; Komaromi, I.; Gomperts, R.; Martin, R. L.; Fox, D. J.; Keith, T.; Al-Laham, M. A.; Peng, C. Y.; Nanayakkara, A.; Gonzalez, C.; Challacombe, M.; Gill, P. M. W.; Johnson, B. G.; Chen, W.; Wong, M. W.; Andres, J. L.; Head-Gordon, M.; Replogle, E. S.; Pople, J. A. *Gaussian 03*, Revision B.1; Gaussian, Inc.: Pittsburgh, PA, 2003.

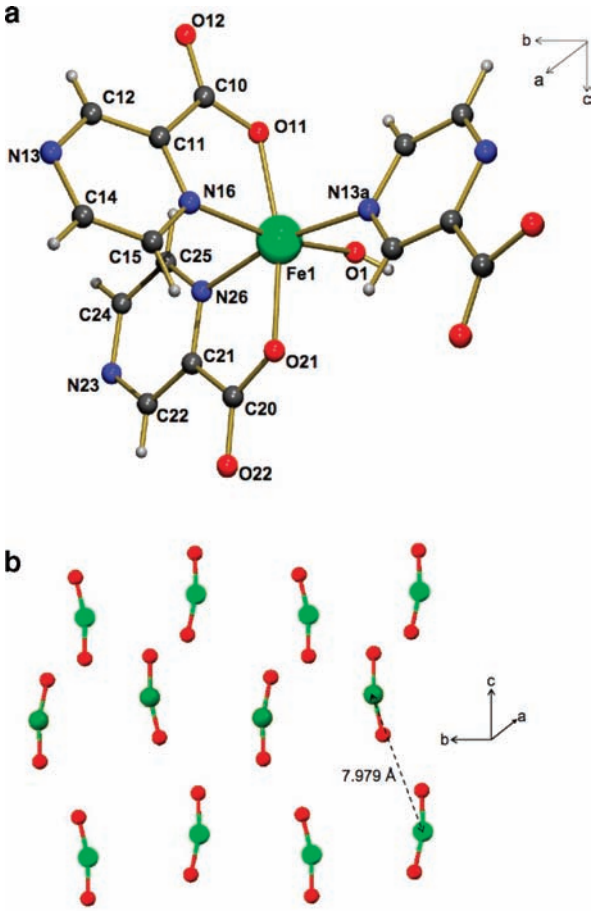

Figure 2. Molecular (a) and partial crystallographic structure, (b) obtained from reference 8, of the $[Fe(pca)_3H_2O]^-$ anion, **2**, in $\{[Fe(pca)_2(H_2O)]\cdot H_2O\}_n$. The iron(II) ion is shown in green, oxygen in red, nitrogen in blue, carbon in black, and hydrogen in gray.

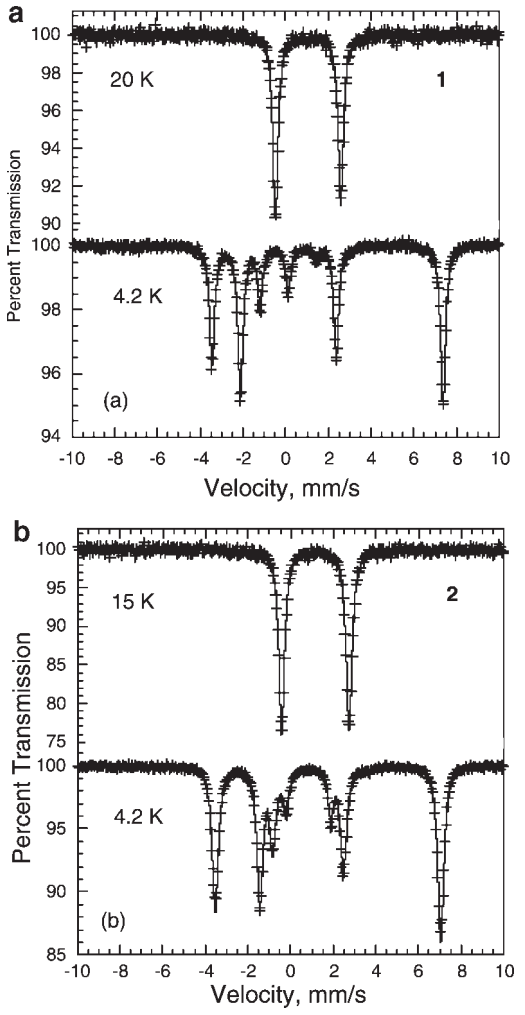

Figure 3. Mössbauer spectra of $[Fe(pca)_2(py)_2]\cdot py$, (a), and of $\{[Fe(pca)_2(H_2O)]\cdot H_2O\}_n$, (b), obtained at 20 or 15 K, above their 12 K antiferromagnetic ordering temperatures, and at 4.2 K, below the ordering temperatures. The complete temperature dependence of the spectra may be found in reference 8.

and two different basis sets. The first basis set, designated as basis set A herein, used the relativistic electron core double-ζ LANL2DZ pseudo potentials[10] for iron(II) in conjunction with the 6-31G(d) basis set for all other atoms. The second basis set, designated as basis set B herein, used the 6-311++G(d,p) basis set for all atoms and ions including the iron(II). Earlier reports[11−13] have indicated that the B3LYP functional is the most reliable for the study of iron(II) complexes.

The lower level calculations with basis set A were carried out first. Subsequently, to improve the accuracy of the results and also to calculate, $\rho(0)$, the s-electron probability density at the iron(II) nucleus, all the calculations were carried out with the larger basis set B, a basis set that includes more diffusion and polarization functions for all atoms and ions. The lower level calculations are included herein to show that they lead to results that are both comparable with the larger basis set and lead to results that are consistent with the experimental Mössbauer spectral hyperfine parameters.

A single point electronic energy computation was used for the single crystal X-ray structures, followed by a Gaussian03 structural optimization. All computations have been carried out for the quintet state, the spin-state that corresponds to the high-spin iron(II) electronic ground state observed for both complexes. The electronic structure calculations have converged to $\pm 1 \times 10^{-8}$ a.u. for the energy and used an ultra fine grid for the computation of the integrals. For the geometry optimizations, all of the vibrational frequencies were positive. The natural orbital populations have been calculated at the same computational level by using the method of Carpenter and Weinhold,[14] and the tensor representation of the electric field gradients have been calculated by the method of Barone.[15] To calculate the iron-57 Mössbauer-effect isomer shifts, the full core electron density, $\rho(0)$, was computed at the iron nucleus with basis set B by using the Gaussian03 cubegen[16] full-density option.

Results and Discussion

The 173 K single crystal X-ray structure of both $[Fe(pca)_2(py)_2]\cdot py$, and $\{[Fe(pca)_2(H_2O)]\cdot H_2O\}_n$, where pca is the 2-pyrazinecarboxylate anionic ligand and py is pyridine, have been reported[8] and found to contain high-spin

(10) Hay, P. J.; Wadt, W. R. *J. Chem. Phys.* **1985**, *82*, 270–283. Hay, P. J.; Wadt, W. R. *J. Chem. Phys.* **1985**, *82*, 299–310.
(11) Havlin, R. H.; Godbout, N.; Salzmann, R.; Wojdelski, M.; Arnold, W.; Schultz, C. E.; Oldfield, E. *J. Am. Chem. Soc.* **1998**, *120*, 3144.
(12) Godbout, N.; Havlin, R. H.; Salzmann, R.; Debrunner, P. G.; Oldfield, E. *J. Phys. Chem. A* **1998**, *102*, 2342.
(13) Zhang, Y.; Oldfield, E. *J. Phys. Chem. A* **2003**, *107*, 4147.
(14) Carpenter, J. E.; Weinhold, F. *J. Mol. Struct., THEOCHEM* **1988**, *169*, 41.
(15) Barone, V. *Chem. Phys. Lett.* **1996**, *262*, 201.
(16) *Gaussian03 User's Reference*; Gaussian, Inc.: Pittsburgh, PA, 2003; p 247.

Table 1. Calculated Iron(II) Natural Charges and Electronic Configurations

complex	structure	basis set	charge	electronic configuration
$[Fe(pca)_2(py)_2]$, **1**	X-ray[a]	A	1.44	$[Ar]4s^{0.25}3d^{6.27}4p^{0.02}4d^{0.01}5p^{0.01}$
		B	1.43	$[Ar]4s^{0.24}3d^{6.26}4p^{0.01}4d^{0.06}$
	optimized	A	1.45	$[Ar]4s^{0.24}3d^{6.27}4p^{0.02}4d^{0.01}5p^{0.01}$
		B	1.43	$[Ar]4s^{0.24}3d^{6.26}4p^{0.01}4d^{0.06}$
$[Fe(pca)_3H_2O]^-$, **2**	X-ray[a]	A	1.42	$[Ar]4s^{0.26}3d^{6.28}4p^{0.02}4d^{0.01}5p^{0.01}$
		B	1.43	$[Ar]4s^{0.25}3d^{6.26}4p^{0.01}4d^{0.05}$
	optimized	A	1.46	$[Ar]4s^{0.24}3d^{6.26}4p^{0.02}4d^{0.01}5p^{0.01}$
		B	1.47	$[Ar]4s^{0.22}3d^{6.25}4p^{0.01}4d^{0.04}$

[a] Structure obtained from reference 8.

iron(II) with a quintet electronic ground state; the molecular structures and partial packing diagrams are shown in Figures 1 and 2. Both complexes are paramagnetic above 12 K, are antiferromagnetically ordered below 12 K, and exhibit[8] fully ordered Mössbauer spectra at 4.2 K, see Figure 3.

The geometry of a single molecule of $[Fe(pca)_2(py)_2]$, **1**, and of a single anion, $[Fe(pca)_3H_2O]^-$, **2**, has been extracted from their unit cells and has been used as the input structure for the calculations reported herein. The electronic structures of the iron(II) quintet state have been computed using two different basis sets, A and B, as delineated in the Computational Methods section above. Subsequently, the X-ray derived structures have been optimized by Gaussian03 to minimize the energy of the quintet state in the gas phase for **1** and **2** with both basis sets. It was verified that all the optimized geometries have real vibrational frequencies.

The calculated electronic properties and the calculated and observed Mössbauer spectral hyperfine parameters for both the X-ray and optimized structures of **1** and **2** are given in Tables 1−3. The calculated natural charges and electronic configurations for the iron(II) are essentially independent of the basis set used and show little change upon optimization. The calculated natural charge on the iron(II) of about 1.45 is essentially the same as observed[17] earlier in several high-spin iron(II) pyrazolylborate complexes.

The calculated total molecular energies are given in Supporting Information, Table S1. Optimization reduces the energy for **1** by about 7.4 eV, a reduction that is similar to that reported for similar calculations[17] on pyrazolylborate complexes. In contrast, optimization reduces the energy for **2** by about 14 eV, a larger reduction that results from the rotation of the water molecule to form a hydrogen bond with the free carboxylate oxygen in one of the pca anionic ligands of **2**.

A comparison of the bond distances of the optimized structures with those of the X-ray structures is given in the Supporting Information, Table S2. In general there are only very small changes in the intraligand bond distances, whereas there is an average elongation of the iron(II) to coordinated ligand atoms of about 0.025 Å for **1** and about 0.050 Å for **2**. The differences between the optimized structure and the results obtained from the X-ray structure, see Supporting Information, Table S2, may be considered to represent the difference between the ideal minimum energy zero Kelvin gas-phase molecular structure and the molecular structure at 173 K in the presence of solid-state lattice interactions.

Electric Field Gradients. The Gaussian03 program determines the electrostatic potential at each atom or ion in a compound and the second derivatives of this potential with respect to distance yield the electric field gradient tensor and, thus V_{zz} and η, at an atom or ion; the corresponding eigenvectors provide the orientation of V_{zz} with respect to a molecular axis.

The principal component of the electric field gradient, V_{zz}, may also be determined experimentally from the quadrupole interaction at the iron-57 nucleus by Mössbauer spectroscopy.[5,6] Thus a comparison of calculated and experimentally observed electric field gradients provides a test of the validity of the computational methods and the modeling of a single molecule in the unit cell, at least for the iron(II) complexes under study. The calculated V_{zz}, ΔE_Q, and η, and the observed ΔE_Q and η for **1** and **2**, are given in Table 2. With one exception, there is good to excellent agreement between the calculated and observed ΔE_Q and η parameters.

The above-noted exception occurs for the optimized structures of the $[Fe(pca)_3H_2O]^-$ anion, **2**, especially the structure optimized with basis set A. The structural optimization leads to a rather large elongation of 0.163 and 0.145 Å for the Fe−O1 bond distance to the coordinated water molecule when using the A and B basis sets, respectively. This elongation mainly results from a hydrogen bonding interaction between the water molecule and the free carboxylate in one of the pca anionic ligands of **2**, an interaction which is absent in the solid-state lattice. In the case of the optimization with basis set B, the elongation of the Fe−O1 bond is accompanied by an increase in the charge on O1 and, as a consequence, the electric field gradient at the iron(II) is only slightly different from that calculated for the X-ray structure.

In earlier work[17] with the same functional and basis sets, the accuracy of the calculated V_{zz} values was estimated to be about ±0.002 a.u. and possibly as good as ±0.001 a.u. The corresponding accuracy of the quadrupole splittings, ΔE_Q, would then be ±0.004 mm/s or better, see Table 2. However, the calculated value of ΔE_Q also depends on the value of the nuclear quadrupole moment, Q, which, unfortunately, is poorly determined; values ranging from -0.19 to $+0.44 \times 10^{-28}$ m^2 have been reported.[13] At present the best experimental value[11−13,18] for Q is $0.16(1) \times 10^{-28}$ m^2, and this value has been used in Table 2. The error of $\pm 0.01 \times 10^{-28}$ m^2 in Q corresponds to an error of ±0.20 mm/s in the calculated values of ΔE_Q, an error that is, of course, constant for all values. As a consequence, Table 2, gives the relative error in ΔE_Q obtained from the Gaussian03 calculation of V_{zz}.

Magnetic Easy-Axis Determination. $[Fe(pca)_2(py)_2]$, **1**, was chosen for the initial magnetic easy-axis determination because, as indicated earlier,[8] it has a pseudooctahedral

(17) Remacle, F.; Grandjean, F.; Long, G. J. *Inorg. Chem.* **2008**, *47*, 4005.

(18) Dufek, P.; Blaha, P.; Schwarz, K. *Phys. Rev. Lett.* **1995**, *75*, 3545.

Table 2. Calculated and Observed Iron(II) Electric Field Gradients and Quadrupole Interactions

		calculated				obs.[a]		
complex	structure/ basis set	V_{zz}, a.u.[b]	$eQV_{zz}/2$, mm/s[b]	η	ΔE_Q, mm/s[b]	ΔE_Q, mm/s	η	θ, deg
$[Fe(pca)_2(py)_2]$, **1**	X-ray[a]/A	−1.800(2)	2.910(4)	0.02	2.92	+3.04(1)	0.0	12
	X-ray[a]/B	−1.696(2)	2.742(4)	0.02	2.75	+3.04(1)	0.0	12
	optimized/A	−1.812(2)	2.930(4)	0.02	2.94	+3.04(1)	0.0	12
	optimized/B	−1.641(2)	2.740(4)	0.02	2.75	+3.04(1)	0.0	12
$[Fe(pca)_3H_2O]^-$, **2**	X-ray[a]/A	−1.849(2)	2.991(4)	0.04	3.01	+3.16(1)	0.0	26
	X-ray[a]/B	−1.719(2)	2.780(4)	0.21	2.88	+3.16(1)	0.0	26
	optimized/A	−1.119(2)	1.809(4)	0.92	2.07	+3.16(1)	0.0	26
	optimized/B	−1.618(2)	2.616(4)	0.16	2.69	+3.16(1)	0.0	26

[a] X-ray structures measured at 173 K and observed values measured at 4.2 K and obtained from reference 8. [b] 1 a.u. is 9.717×10^{21} V/m^2 and corresponds to an $(eQV_{zz})/2$ of 1.617 mm/s, if the nuclear quadrupole moment is $0.16(1) \times 10^{-28}$ m^2. The error given for $(eQV_{zz})/2$ is the computational error. The error including the error in the nuclear quadrupole moment would be ±0.20 mm/s.

Table 3. Calculated *ns*-Electron Probability Densities at the Iron-57 Nucleus[a]

complex	structure/ basis set	$\rho(0)$, a_0^{-3}	δ,[a] mm/s observed at 295 K	δ,[a] mm/s observed at 4.2 K
$[Fe(pca)_2(py)_2]$, **1**	X-ray[b]/B	11614.622	1.229(5)	1.312(5)
	optimized/B	11614.490	1.229(5)	1.312(5)
$[Fe(pca)_3H_2O]^-$, **2**	X-ray[b]/B	11614.498	1.303(5)	1.410(5)
	optimized/B	11614.342	1.303(5)	1.410(5)

[a] The isomer shifts are given relative to room temperature sodium nitroprusside, SNP. [b] Structure obtained from reference 8.

FeO_2N_4 coordination environment in which the two carboxylate oxygens occupy the *trans* positions. Thus, it would be anticipated that one or the other of the almost collinear Fe−O18 and Fe−O28 bond directions, directions that make angles of 21.8° and 13.4° with the crystallographic *c*-axis of **1**, or their average would correspond, at least rather closely, to the axis of the principal component, V_{zz}, of the electric field gradient tensor at the iron(II) ion.

DFT calculations on **1** indicate that V_{zz} makes an angle of 14° with the *z*-axis used internally by Gaussian03 and the Fe−O18 and Fe−O28 bond directions make angles of 17.2° and 16.5° with this *z*-axis. Hence, the calculated V_{zz} of the electric field gradient tensor is indeed close to the almost collinear Fe−O18 or Fe−O28 directions in **1**. More specifically the Fe−O28 direction makes an angle of 2° with the calculated V_{zz} axis. Thus, V_{zz} is along the Fe−O28 direction, a direction which makes an angle of 13.4° with the crystallographic *c*-axis.

A fit of the magnetic Mössbauer spectra of **1** indicates that the magnetic hyperfine field lies on a cone with a cone angle of 12° about V_{zz}. Hence, the magnetic moment, which is assumed to be collinear with the magnetic hyperfine field at the iron-57 nucleus, lies on the same cone and is likely to be parallel or virtually parallel with the crystallographic *c*-axis of **1**.[19] As can be seen in Figure 1b, the *c*-axis is the bisector of the O18−O28 directions of adjacent molecules along the *b*-axis.

As indicated earlier,[8] it is much more difficult to predict the orientation of V_{zz} in **2**. The DFT calculations indicate that V_{zz} makes angles of 86.8°, 30.2°, and 59.9°, with the *x*, *y*, and *z* internal molecular axes used by Gaussian03, respectively. This V_{zz} direction, which makes angles of 75.3°, 86.6°, and 14.9°, with the *a*, *b*, and *c* unit-cell axes, is almost coincident with the O11−Fe−O21 axis, as proposed earlier.[8] Thus it seems that the presence of water in the coordination sphere of **2** neither determines the orientation of V_{zz} nor leads to a substantial asymmetry parameter, η.

A fit of the magnetic Mössbauer spectra of **2** indicates that the magnetic hyperfine field lies on a cone with a cone angle of 26° about V_{zz}. The angles between V_{zz} and the unit-cell axes do not correspond to this angle and thus, it appears that none of the unit-cell axes could be the magnetic easy-axis of **2**. In contrast, and perhaps by coincidence, V_{zz} makes an angle of 26.1° with the Fe···Fe distance of 7.979 Å, see Figure 2b. Hence, we conclude that the magnetic easy-axis in **2** may be along this Fe···Fe direction. It is surprising that this is not the direction of the shortest Fe···Fe distance.

Electron Probability Density at Iron(II). The Mössbauer-effect isomer shift provides a measure of the s-electron probability density at the iron-57 nucleus relative to that found in either α-iron or sodium nitroprusside, SNP, the typical reference materials for the iron-57 Mössbauer-effect isomer shift. This s-electron probability density is influenced both by the *ns*-orbital electronic populations and by the shielding of this *ns*-electron probability density by the intervening 3d electrons.[20−26]

(19) This conclusion seems to contradict the previous, now known to be erroneous, conclusion given in reference 8 that the *a*-axis of **1** was the magnetic easy-axis. This earlier error occurred because of a mislabeling of the axes at the left of Figure 2(a) of reference 8.

(20) Neese, F. *Inorg. Chim. Acta* **2002**, *337*, 181.
(21) Nieuwpoort, W. C.; Post, D.; Van Duinen, P. Th *Phys. Rev. B* **1978**, *17*, 9.
(22) Lovell, T.; Li, J.; Liu, T.; Case, D. A.; Noodleman, L. *J. Am. Chem. Soc.* **2001**, *123*, 12392. Lovell, T.; Han, W.-G.; Liu, T.; Noodleman, L. *J. Am. Chem. Soc.* **2002**, *124*, 5890.
(23) Shenoy, G. K.; Wagner, F. E.; Kalvius, G. M. In *Mössbauer Isomer Shifts*; Shenoy, G. K., Wagner, F. E., Eds.; North Holland: Amsterdam, 1978; p 51.
(24) Owen, T.; Grandjean, F.; Long, G. J.; Domasevitch, K. V.; Gerasimchuk, N. *Inorg. Chem.* **2008**, *47*, 8704.
(25) Neese, F. *J. Biol. Inorg. Chim.* **2006**, *11*, 702.
(26) Zhang, Y.; Mao, J.; Oldfield, E. *J. Am. Chem. Soc.* **2002**, *124*, 7829–7839. Zhang, Y.; Oldfield, E. *J. Phys. Chem. A* **2003**, *107*, 4147–4150. Zhang, Y.; Oldfield, E. *J. Phys. Chem. A* **2003**, *107*, 7180–7188.

The electron probability density, $\rho(0)$, at the iron-57 nucleus of **1** and **2** has been calculated from the Gaussian03 derived wave functions, and the results are given in Table 3. A pseudopotential cannot be used to calculate $\rho(0)$ at the iron(II) ions and, as a consequence, the $\rho(0)$ values found in this table must be calculated by using the 6-311++G(d,p) basis set, the basis set designated as B herein, for all the constituents including the iron(II). Rather nicely, the calculated $\rho(0)$ values correspond very closely to those expected for high-spin iron(II) and indeed agree very nicely with earlier DFT calculations on several high-spin and low-spin iron(II) complexes, see Figure 4a. The correlation between the observed isomer shifts and the calculated $\rho(0)$ values is

$$\delta_{SNP} = -0.368[\rho(0) - 11617.63] \text{ mm/s}$$

or

$$\delta_{SNP} = -0.0546[\rho(0) - 78390.40] \text{ mm/s}$$

where, in the first equation, the probability density, $\rho(0)$, has units of a_0^{-3} and in the second equation, see Figure 4a, the probability density, $\rho(0)$, has units of $Å^{-3}$.

In spite of a smaller isomer shift range of 0 to 1.5 mm/s and smaller change in $\rho(0)$ of about 3.5 a_0^{-3}, the slope of the straight line in the first equation, -0.368 a_0^3mm/s, agrees almost perfectly with the slope of -0.36662 a_0^3mm/s obtained by Neese[20] in his calibration of the B3LYP method with 15 iron containing compounds, see Figure 4b. This excellent agreement indicates that the calibration constant for the B3LYP method is well-defined as is indicated by the difference in the solid and dashed lines in this figure. As indicated by Neese[20] the absolute values of $\rho(0)$ obtained with various functionals and wave function basis sets show a significant dispersion but their variations within a series of compounds are chemically and physically meaningful. The comparison of the $\rho(0)$ obtained herein with the fifteen values reported by Neese in Figure 1 of reference 20 required a shift of -1445 $Å^{-3}$ to obtain the agreement shown in Figure 4b, a relatively small shift of about 1.8% that probably arises from differences in the basis sets used.

Zhang and Oldfield[26] have used the B3LYP functional to determine the Mössbauer spectral hyperfine parameters of many compounds, and in several instances, have reported the associated $\rho(0)$ at the iron-57 nucleus. Their reported $\rho(0)$ values, converted to the same units used in Figure 4a, are compared in the Supporting Information, Figure S1, with the linear correlation obtained herein. Once again there is excellent agreement between the two correlations, although in this case the linear correlation yields -0.400 a_0^3mm/s, a value in good agreement with the value of -0.404 a_0^3mm/s found in many studies by Zhang and Oldfield. In obtaining the agreement shown in Supporting Information, Figure S1 a shift of -90 $Å^{-3}$ or of only 0.1% has been applied to the results of Zhang and Oldfield, a much smaller shift than used in Figure 4b because of their use[26] of basis sets that are very similar to those used herein.

The calibration constant of -0.368 a_0^3mm/s found herein agrees rather well with other previously reported results.[12,17,21] The calibration constants of about

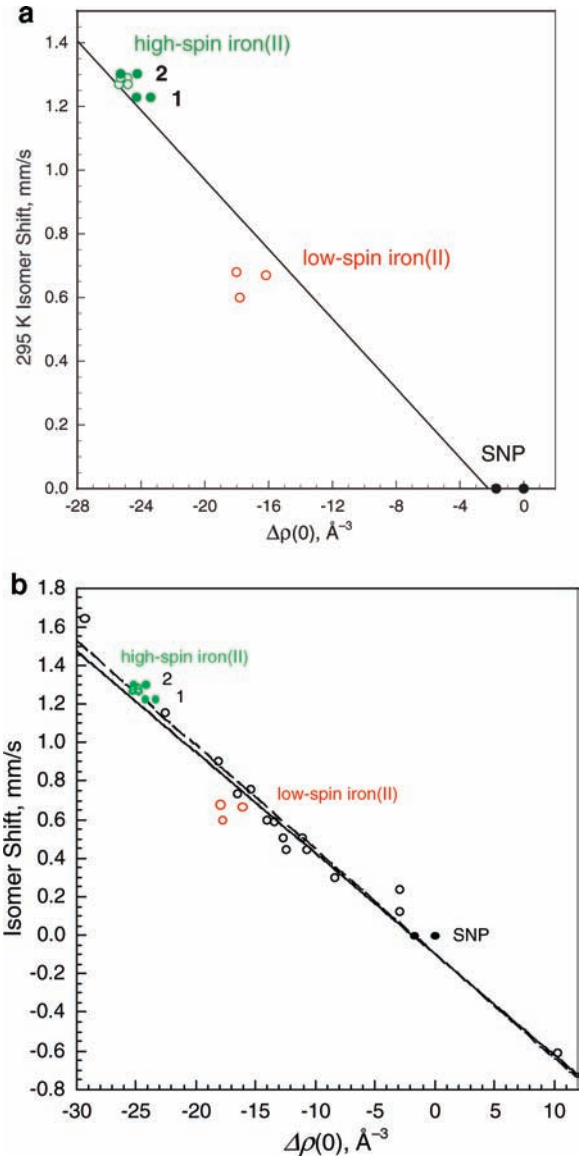

Figure 4. (a) Correlation observed between the 295 K Mössbauer spectral isomer shifts and $\rho(0)$, the calculated *ns*-electron probability densities at the iron(II) in $[Fe(pca)_2(py)_2]$, **1**, of $[Fe(pca)_2(py)_2]\cdot py$, and in the $[Fe(pca)_3H_2O]^-$ anion, **2**, of $\{[Fe(pca)_2(H_2O)]\cdot H_2O\}_n$. The isomer shifts are given relative to sodium nitroprusside, SNP; the right SNP data point was obtained for its crystal structure and the left for its optimized structure, see reference 17. The open data points, which correspond to several high-spin and low-spin iron(II) pyrazolylborate complexes, have been taken from reference 17 which also identifies the specific complexes. (b) The same correlation observed between the Mössbauer spectral isomer shifts and $\rho(0)$, the calculated *ns*-electron probability densities as is shown in panel a, but with the addition of the correlation, dashed line, derived by Neese in reference 20, based on the open black points. The identity of the compound associated with each of the open black points is given in reference 20. The isomer shifts reported relative to α-iron and used by Neese are given relative to sodium nitroprusside by the addition of 0.26 mm/s.

-0.5 and -0.664 a_0^3mm/s obtained by Lovell et al.[22] in Fe−S systems and 15 dinuclear Fe-oxo, Fe-hydroxyl, and Fe-phenoxo type compounds differ from the present value because a different functional and wave function basis set were used. The correlation presented in Figure 4a supports[20] the good quality of the prediction of the relative Mössbauer isomer shifts based on DFT calculation of $\rho(0)$ in a series of compounds. Further, the isomer shifts are calculated relative to the SNP Mössbauer-effect

reference standard by using exactly the same functional and basis set.

Infrared Spectra. The infrared spectra of **1** and **2** have been measured between 4000 and 300 cm^{-1} and between 600 and 150 cm^{-1}; the 1800 to 300 cm^{-1} portions of these spectra are shown in the Supporting Information, Figure S2.

The frequencies and relative intensities of the $3n - 6$, or 135 and 114, normal coordinate vibrational modes available to **1** and **2**, respectively, were computed for the equilibrium and X-ray geometries. When the electronic structure computation is constrained to the X-ray structure some of these vibrational modes are found to have imaginary frequencies because the X-ray geometry is not a minimum for an isolated molecule in the gas phase. However, this was not the case after geometry optimization: for both **1** and **2** all the vibrational frequencies were real as reported above. Of course most of the vibrational modes involve multiple atoms and several types of vibrations but, in conjunction with the observed infrared spectra of the complexes, some general conclusions may be reached based on the normal coordinate vibrational analysis. These conclusions are discussed in some detail in the Supporting Information.

Some insight into the vibrational behavior of the iron-57 nucleus can be obtained from the temperature dependence of the isomer shift. The temperature dependence[8] of the isomer shift of **1** has been fit with the Debye model[23] for the second-order Doppler shift and a Mössbauer temperature of 641(22) K has been obtained, a temperature which is an approximate measure[24] of the energy of the high-frequency phonons associated with the iron(II) vibrations. The 314 cm^{-1} weighted average of the iron(II) vibrational frequencies obtained from the DFT calculations, see the Supporting Information, corresponds to 450 K, a temperature that is of the order of the Mössbauer temperature. The highest calculated iron(II) vibrational frequency of 430 cm^{-1} corresponds to 620 K, a temperature that is in good agreement with the observed Mössbauer temperature. DFT calculations of vibrational frequencies are known[25] to overestimate vibrational frequencies by a few percents as compared to experimental values. Moreover, the harmonic approximation is used for the normal modes, and their anharmonicities have not been taken into account. Hence, a detailed comparison between the calculated and observed iron(II) vibrational frequencies is hindered by these limitations.

Because the calculated vibrational modes of **2** are strongly affected by the presence of the water molecule and the hydrogen bonding found in the optimized structure, a similar comparison has not been attempted for **2**.

Conclusions

DFT calculations with the B3LYP functional and the 6-311 + + G(d,p) basis set yield s-electron probability densities and electric field gradient tensors for an iron(II) ion that are in excellent agreement with the observed iron-57 Mössbauer spectral isomer shifts and quadrupole interactions. Further, a combination of DFT calculations and Mössbauer spectroscopy may be used to determine the magnetic easy-axis of a magnetically ordered iron(II) complex.

The use of the B3LYP functional and the 6-311 + + G(d,p) basis set for all atoms or the simpler, less computer time demanding, relativistic electron core double-ζ LANL2DZ pseudopotential for iron(II) and the 6-31G(d) basis set for all other atoms lead to very similar electric field gradient tensors for the iron(II) ion but, unfortunately, the pseudopotential is unsuitable for the calculation of the s-electron probability density at an iron(II) ion.

Herein we have studied two high-spin iron(II) complexes that do not show any evidence[8] for a spin-state crossover at or below 295 K. Thus, it is indeed satisfying that the present calculations yield very realistic electric field gradients just as they have for several complexes that do show a spin-state crossover.[11,12,17,26] Further, it is worth noting that the calculations yield for these complexes $\rho(0)$ values, and hence isomer shifts, that are very close to those observed previously, see the green points in Figure 4a, for several high-spin complexes[17] that do undergo a spin-state crossover; good agreement is also observed[11,12,20,25,26] with other high-spin iron(II) complexes.

The calculated gas phase s-electron probability density and electric field gradient tensor for an iron(II) ion are very similar for calculations based on either the experimental X-ray structure or on the optimized structure obtained after minimizing the molecular energy starting from the X-ray structure. The optimization does, however, lead to structures in which the iron(II) to ligand bond distances have increased as a result of the absence of any solid-state lattice interactions. Also, upon optimization all the calculated normal coordinate vibrational modes are found to have positive frequencies, frequencies that agree rather well with those observed in the infrared spectra.

Acknowledgment. The quantum chemistry computations have been carried out at the University of Liège with the support of F.RFC 9.4545.03F and 2.4.565.06.F (Belgium), and the Ministère de la Région Wallonne with grant RW/115012. F.R. is a Director of Research from FNRS (Belgium). G.P. is a postdoctoral fellow of the AIP project of the Belgian federal government: Quantum effects in clusters and nanowires.

Supporting Information Available: Table S1, the calculated total molecular energies and Table S2, the X-ray and optimized molecular structures. Figure S1, a comparison between correlations of $\rho(0)$ with the isomer shift and Figure S2, the infrared spectra of **1** and **2**. This material is available free of charge via the Internet at http://pubs.acs.org.